

*Master in Photonics*

**MASTER THESIS WORK**

**Microwave Photonic Filter with Independently Tunable  
Cut-Off Frequencies**

**Tamas Gyerak**

**Supervised by Dr. Maria Santos, (UPC)**

Presented on date 14<sup>th</sup> July 2016

Registered at

 Escola Tècnica Superior  
d'Enginyeria de Telecomunicació de Barcelona

## ABSTRACT

A simple technique for microwave photonic filtering is presented, which allows independent tunability of each end of the RF passband by tuning of the wavelengths of the lasers which are phase modulated with the RF signal and optically filtered. The results proved its potential and the conducted research has revealed the key role played by the optical filter spectral transfer characteristics.

## 1. INTRODUCTION

### 1.1 Motivation

Microwave photonics is a research area that is focused on photonic subsystems designed for applications dealing with signals in the microwave domain. The term microwave will be freely used throughout this paper to refer to systems dealing with signals whose wavelength is comparable with their size. Microwave photonics are used in conditions where reducing the weight and volume and providing high level of tunability and reconfigurability are important. Nowadays, this field of technology witnesses great amount of research and investments due to the increasing demand of the market. For example, satellite system applications are starting to require THz capacity as well as advanced signal processing that can be performed on such photonic systems. Spectral band selection and filtering techniques are the main issues when physical units have to perform the signal processing on-board communications and Earth observation satellites.

### 1.2 State of the Art

Microwave photonic filtering techniques can be broadly categorized into two areas: coherent and incoherent schemes. Coherent schemes have no phase induced incoherent noise. For incoherent schemes usually a lot of taps are required so that their complexity increases, see Ref [1].

The present work focuses on coherent techniques, specifically those using PM to IM conversion through optical filtering of one of the sidebands. The principle operation of a PM to IM conversion scheme is as follows. Firstly, a basic EM wave enters the system from a laser output:

$$E = \text{Re}\{E_0 \exp(i\omega t + i\phi_0)\} \quad (1)$$

This wave is phase modulated with the microwave signal at frequency  $\omega_m$ :

$$E = \text{Re}\{E_0 \exp(i\omega t + i\phi_0) [J_0(A) + J_1(A) \exp(i\omega_m t) - J_1(A) \exp(-i\omega_m t)]\} \quad (2)$$

Where J is a Bessel function with A being the phase modulation index and  $V_\pi$  being the PM's half-wave voltage:

$$A = \frac{V}{V_\pi} \pi \quad (3)$$

Assuming low modulation index, so that only one sideband is taken into account.

Optical detection is typically square-law detection, so that the detected photocurrent is obtained as

$$I(t) = I_{dc} + J_0(A) J_1(A) E_0^2 [\cos(\omega_m t) - \cos(\omega_m t)] \quad (4)$$

If one sideband is taken out by optical filtering, leaving the carrier and one sideband to be detected, the photocurrent is:

$$I(t) = I_{dc} + J_0(A) J_1(A) E_0^2 [\cos(\omega_m t)] \quad (5)$$

An RF signal is therefore detected; providing the RF filtering effect.

<http://www.photonicsbcn.eu>

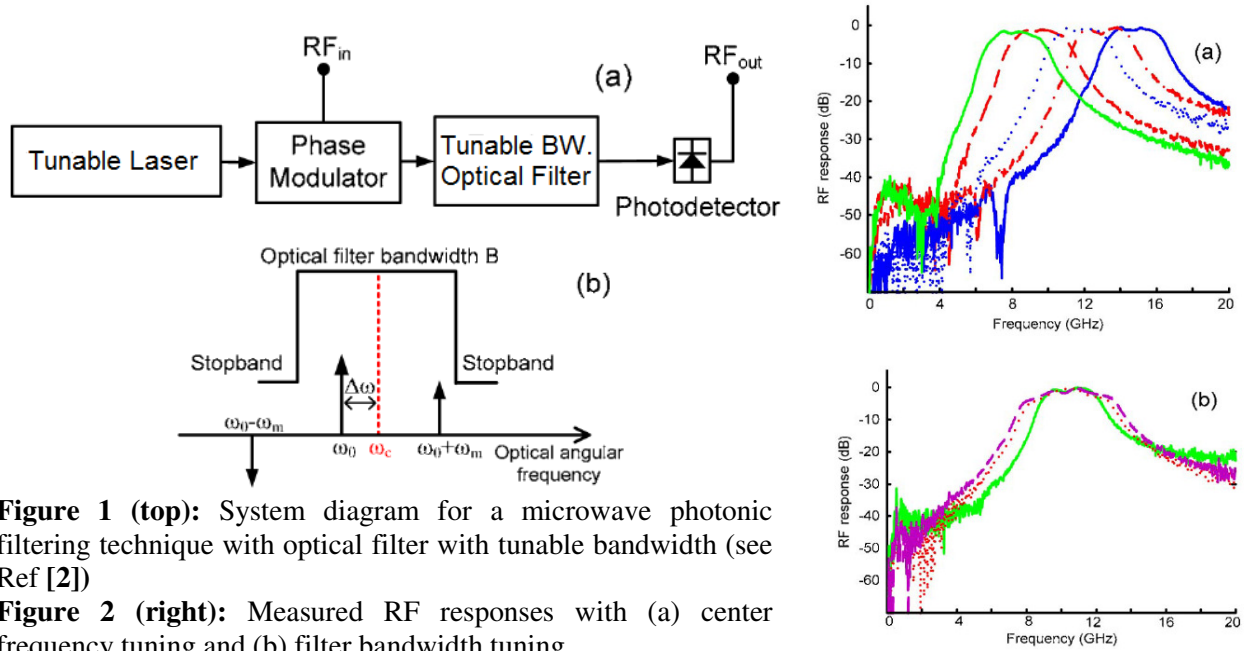


**Figure 1 (top):** System diagram for a microwave photonic filtering technique with optical filter with tunable bandwidth (see Ref [2])

**Figure 2 (right):** Measured RF responses with (a) center frequency tuning and (b) filter bandwidth tuning

An example of coherent microwave photonic filtering through PM to IM conversion is given in Ref [2]. The system follows the scheme in Fig. 1. In this case, the frequency of a tunable laser is selected to lie a distance  $\Delta\omega$  from the center frequency of an optical passband filter as seen in Fig. 1/b. For low modulation frequencies, both sidebands lie within the optical filter passband and therefore no RF signal is photodetected as explained above. As the modulation frequency is increased, one sideband moves out of the optical filter's passband, the lower sideband in the example in Fig. 1/b, yielding a photodetected RF signal. If the modulation frequency keeps increasing the remaining sideband moves out of the optical filter passband as well, and then again no RF signal is detected. That provides the RF passband responses seen in Fig 2. According to the above,  $f_{cl}$  and  $f_{ch}$  at the cut-off frequencies in the lower and higher cut-offs accordingly:

$$\begin{aligned} f_{cl} &= B/2 - \Delta\omega \\ f_{ch} &= B/2 + \Delta\omega \end{aligned} \quad (6)$$

The center of the passband is located at:

$$f_c = (f_{ch} + f_{cl}) / 2 = B/2 \quad (7)$$

Where the bandwidth of the RF filter is:

$$B_{RF} = f_{ch} - f_{cl} = 2\Delta\omega \quad (8)$$

Therefore, changing the laser detuning against the optical filter center frequency,  $\Delta\omega$ , changes the bandwidth of the RF filter and on the other hand, as shown in (7), by temperature tuning the optical filter bandwidth (B) the center frequency of the RF filter is changed. The results in Fig. 2 prove that changing the bandwidth of the optical filter with fixed laser wavelength varies the center frequency electrically, see Fig 2/a. Vice versa, changing the tunable frequency wavelength of the laser with fixed optical filter bandwidth changes the bandwidth electrically, see Fig 2/b. This idea will be utilized in the principle of operation of the MPF technique proposed in the present work.

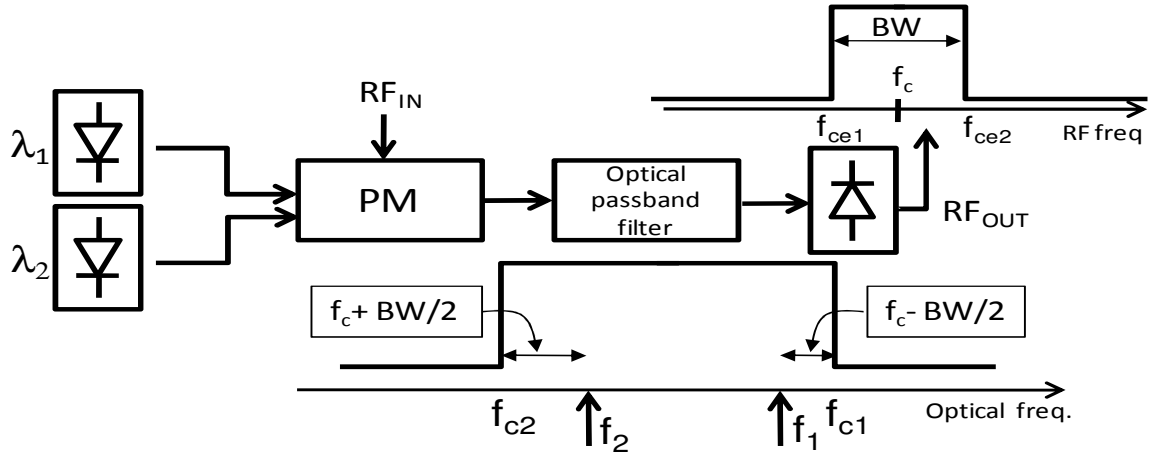


**Figure 3:** System diagram for MPF with two lasers applied

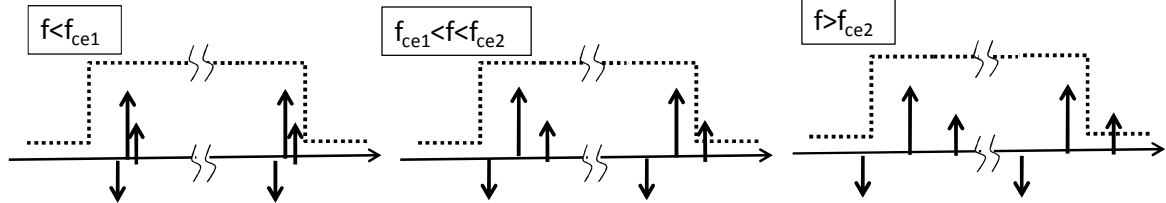


**Figure 4:** Sketch of optical spectrum of PM output relative to optical filter spectrum transfer function for different electrical frequency margins

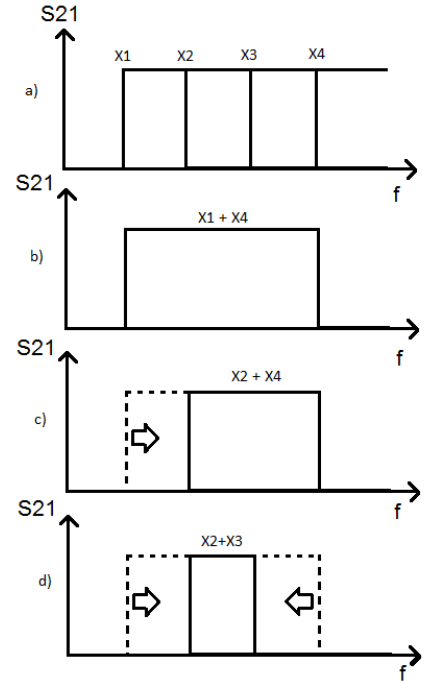
### 1.3 Principle of Operation

Fig. 3 shows the system design for the proposed method to create the MPF with independently tunable cut-off frequencies. Two lasers are used with their output beam's wavelengths set to be within the passband of an optical filter. The lasers are optically coupled and lead into a phase modulator (PM) that inscribes the microwave input signal on both carriers. These modulated signals are then optically filtered and finally detected by a photodetector. The detector can only detect the envelope fluctuations of the received signal, therefore when both signals are inside the passband, along with their sidebands, no electrical signal leaves the detector.

The carrier wavelengths ( $f_2, f_1$ , with  $f_2 < f_1$ ) are selected on purpose to be located relatively close to each of the cut-off wavelengths of the optical filter ( $f_{c2}, f_{c1}$ , with  $f_{c2} < f_{c1}$ ). Their detunings to the neighboring cut-offs are designed to be different compared to each other:  $\Delta f_1 = f_{c1} - f_1 \neq \Delta f_2 = f_2 - f_{c2}$ . The spectral difference,  $f_2 - f_1$ , has to be large enough so that beating of the signals, which come from different lasers, is avoided, or at least it falls outside of the band of interest.

As depicted on Fig. 4, the MPF passband frequency cut-offs will be found with the following equations:  $f_{ec1} = \min(\Delta f_1, \Delta f_2)$ ,  $f_{ec2} = \max(\Delta f_1, \Delta f_2)$ . As the frequency is varied, it is clear that when  $f < f_{ec1}$ , the whole spectrum falls within the passband of the optical filter, however, when the frequency is increased so that  $f_{ec1} < f < f_{ec2}$  one sideband falls out of the passband, therefore envelope fluctuations occur which yield microwave electronic power when the signals are photodetected. Increasing the frequency further,  $f > f_{ec2}$  is reached, where both carriers lose a sideband each, therefore the remaining sidebands cancel each other out if the power levels are kept stable and equal to each other; no electrical fluctuation is noticed.

**Figure 5:** Independent tuning of the cut-off frequencies: a) all four signals of one laser's responses visualized with X1 and X2 are chosen from the lower cut-off of the optical filter and X3 and X4 are from the higher cut-off b) filter transfer function with two lasers applied with signal summation of X1 and X4 c) moving the lower side of the microwave filter by adding X2 to X4 instead of X1 d) tuning the higher side of the filter independently by adding X2 to X3.



### 1.4 The Objective

With the filtering system presented in Fig. 1, the main idea behind this paper is to prove the feasibility of the above presented technique for independent tunability of both ends of the RF passband of the RF filter. Firstly, the RF transfer function for one laser at either the lower cut-off or at the higher cut-off of the optical filter will be obtained. Because the filter has a wide bandwidth, setting the laser close to one of the cut-off creates a high-pass RF characteristic. Depending on the cut-off selected, the detected RF signal will have 180° difference, as the sideband inside the optical filter will have a different sign.

In the example shown in Fig. 5, X1 and X2 represent the one-laser RF transmission parameter S21 as obtained with the laser wavelengths close to the low frequency cut-off of the optical filter,  $f_1 < f_2$  while X3 and X4 correspond to laser wavelengths close to the high frequency cut-off of the optical filter,  $f_4 < f_3$ . Provided the optical filter passband is wide enough so that each one of the two lasers may be placed close to each one of the cutoffs and be detected independently on a single detector, the two laser response of the MPF may be obtained by just adding up the one-laser responses corresponding to each one of the cutoffs. In the example of Fig. 5 by adding X2 and X4 we obtain a wide bandwidth response seen in Fig. 5/c. If we now change X2 by X1, only the lower frequency cutoff is changed, while if we replace X4 by X3 it is the high frequency cutoff the one that gets altered. Therefore the present strategy to prove the feasibility of the setup in Fig. 5 will be based on experimentally measuring the one-laser high pass responses with laser wavelengths located either at the lower or at the higher frequency cut-offs of the optical filter, and then adding them together with the appropriate amplitude weighting that allows to prove the passband filtering and tuning capabilities of the system.

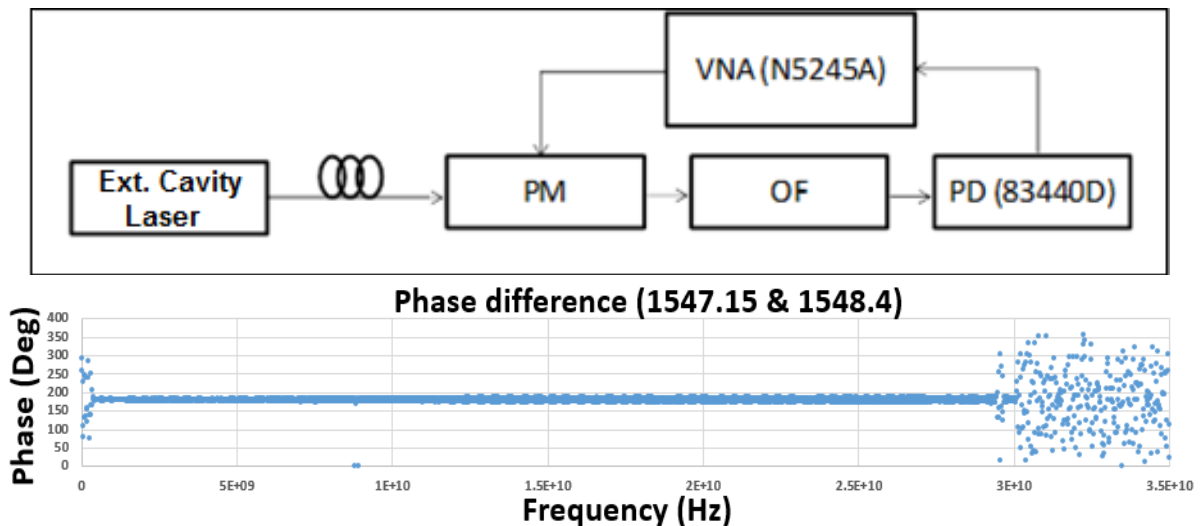


**Figure 6 (above):** Experimental set-up **Figure 7 (below):** Phase difference plot

## 2. EXPERIMENTAL PROCEDURE

As explained above, the filtering technique to be demonstrated involves simultaneous detection of the RF signals modulated over two different lasers at enough spectral distance that the RF signal carried by each one is detected independently and added up at the photodiode's output. One laser needs to stay close to one of the cut-offs of the optical filter and the other close to the other. In order to prove the technique, the goal in this work is to show that the addition of the RF signals obtained using a single laser tuned near one or the other optical filter cut-off when properly post-processed may give rise to the desired tunability of the MPF cut-offs. This would be a fundamental step in order to see and understand the conditions in which the MPF can be realized using two lasers simultaneously.

### 2.1 System analysis

A *New Focus inc.* external cavity laser module was used for the tunable light source, which provides a maximum power of 7dBm. A polarization controller was utilized to control the polarization dependence of the 40 GHz LiNbO<sub>3</sub> phase modulator used to create the RF sidebands with the VNA (N5245A) connected to it. An optical filter was used with nominal central frequency at 1547.72nm. *Hewlett Packard 83440D Lightwave Detector* with nominal 32 GHz band detected the signal with a necessary bias T-connector whose maximum operating frequency was 18 GHz.

Fig. 7 visualizes how the differences of the two S21 phases created by the PM and the optical filter at the two cut-offs was at 180° of phase difference.

The optical filter's transfer function with a resolution bandwidth of 0.1nm of the spectrum analyzer can be seen on Fig. 8.

It is important to analyze the optical filter's response from the VNA as well, in terms of peak amplitude values recorded by the VNA's S21. Fig. 9 shows this; an indicative of the RF response of the microwave photonic filter against different wavelengths. It shows the highest peaks seen on the RF frequency sweep for different wavelengths. It depicts the effect that the signal is detected only when one of the sidebands is filtered.

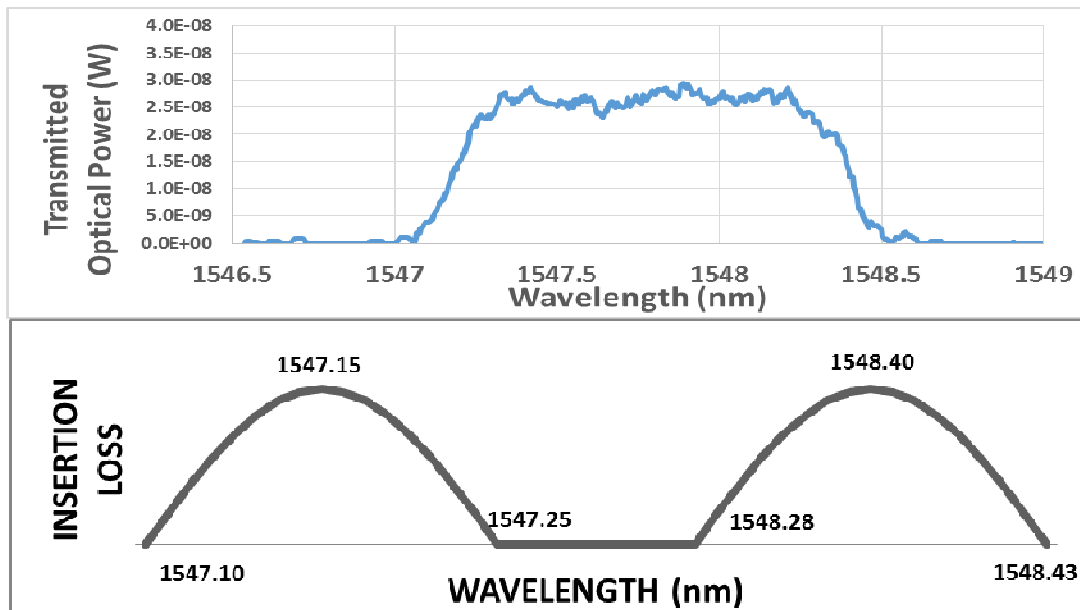


**Figure 8 (above):** Optical Filter Transfer Function **Figure 9 (below):** Value of the maximum peak insertion loss as a function of the laser's wavelength between 1547.10nm-1548.43nm.

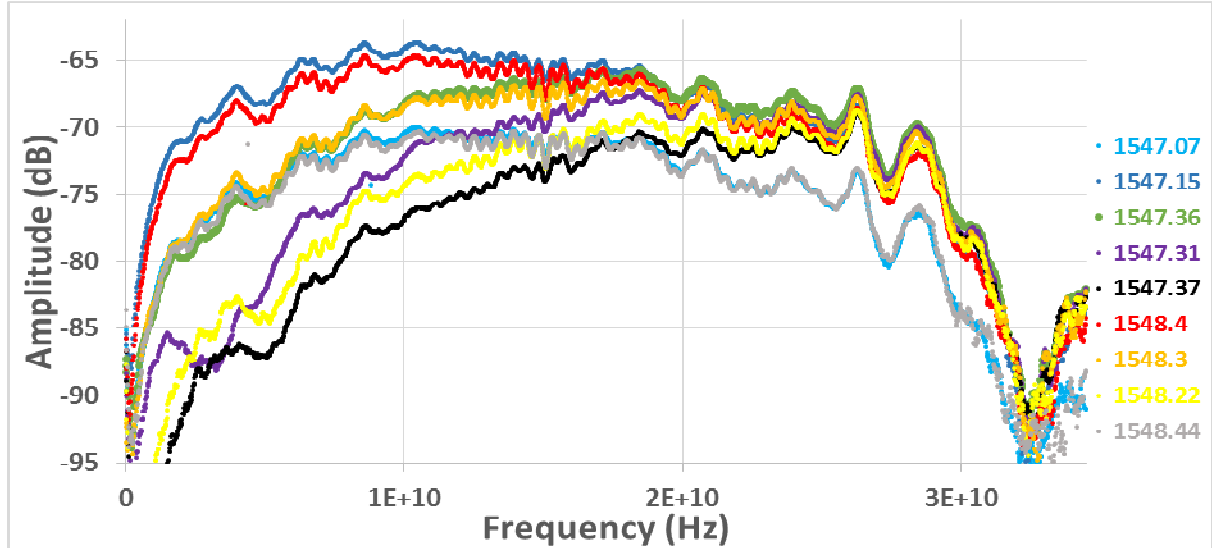


**Figure 10:** Recorded MPF spectral transfer functions for different laser wavelength detunings ( $\Delta f_1, \Delta f_2$ ) from the optical filter center frequency passband, with the VNA's frequency span running from 10MHz to 35GHz with 2000 sampling points recorded

Detection of the signal only appears in the VNA when the carriers are in the slopes of the optical filter's transfer function; when part of the spectrum is taken out. At 1547.15nm and 1548.40nm the highest magnitudes were detected.

## 2.2 Result Analysis I

The whole system creates a PM-IM conversion effect. This type of modulation generates the final recordings for each carrier wavelength positions. Fig 10 shows a number of such VNA recordings taken, where values starting with 1547nm are in the lower cut-off and values starting with 1548nm are for the higher cut-off. This figure is useful to be analyzed with Fig 7 together because while Fig 10 shows the amplitude changes in terms of the varying frequencies, Fig 7 shows the phase variations between two signals that helps with the understanding of how much of the frequency spectra is actually containing information, where noise disturbs the signal, and where the signal completely disappears. From the datasheet of the used equipment the following limits are known even before the experiment. The phase modulator has a bandwidth of 40GHz, so that should not limit the operation. While in Ref. [3], O. Yosefi used a photodetector (PD) with a bandwidth of 10GHz, this system runs on a 32GHz bandwidth PD. However, the most limiting circuit components are the SMA connector as it only functions until 20GHz and the bias T-connector is used for the photodetector that has a 0.1-18GHz passband.

The practical results presented by the amplitude and phase difference figures (Fig. 7 & 10) confirm the expected high-pass behavior for the one laser RF transfer functions. It also shows that the system operating frequency margin extends up to approximately 20 GHz. We also see that the frequency for which the PM to IM conversion takes place is higher the larger the detuning from the optical filter cutoff, as expected. Furthermore, it was proven during the experiment that comparing Fig. 10 to more phase diagrams provides important information about how the circuit behaves at different wavelengths.

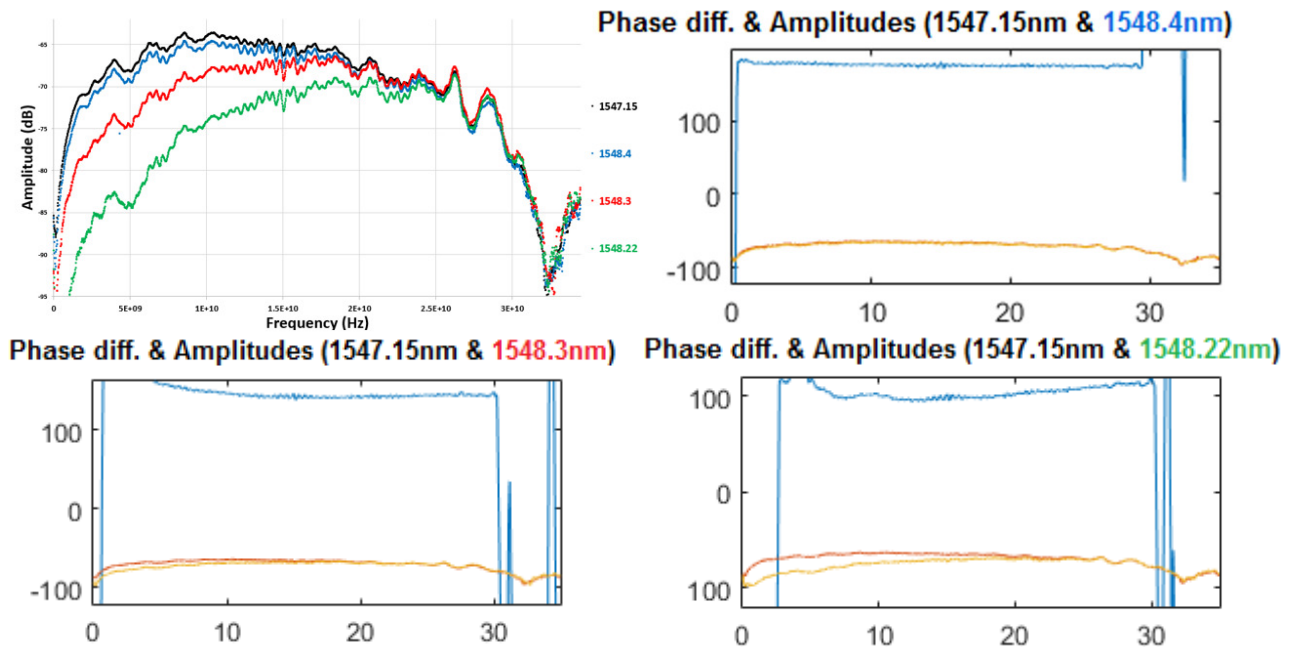


**Figure 11:** Phase difference variations by amplitude differences: the farther away from detuning the farther the phase moves from  $180^\circ$  difference. (Top left) Amplitude curves of the analyzed wavelengths. Amplitude differences (in yellow) and phase differences (blue) plotted with vertical axis being the phase (in degrees) and horizontal axis being the sweep frequency (in GHz) for 1547.15nm taken from the lower cut-off and 3 wavelengths chosen from the higher cut-off: (top right) 1548.4nm, (bottom left) 1548.3nm, (bottom right) 1548.22nm

### 2.3 Result Analysis II

Although the phases of the two peak amplitude values of the two cut-offs proved a very clear  $180^\circ$  difference between the two signals with less than 10% fluctuation from that difference (see Fig 11), the experimental results proved that the optical filter's phase characteristics are not the same throughout its passband.

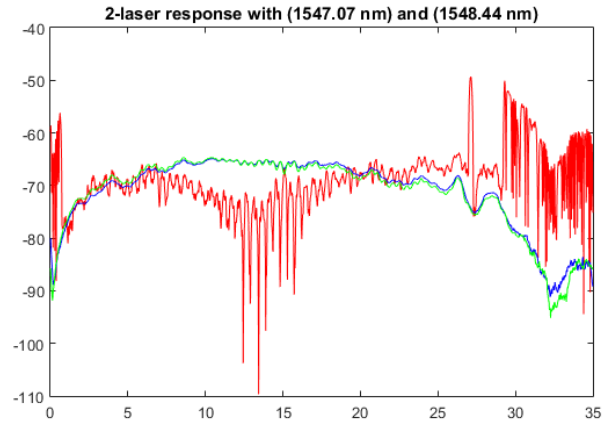
Fig 11 shows that while the phase difference between 1547.15nm and 1548.4nm is at  $180^\circ$ , choosing another wavelength in the place of the 1548.4nm changes this value. As a wavelength is picked in the higher cut-off that has an amplitude peak further away from the recorded 1547.15nm curve, the farther the phase difference moves from the  $180^\circ$  between the wavelengths at different cut-offs. The recorded values for the phase differences are  $174.9^\circ$ ,  $141.3^\circ$ ,  $97.9^\circ$  for 1548.4nm, 1548.3nm, 1548.22nm accordingly.

### 2.4 Result Analysis III

The desired cancellation effect for control of the high frequency cut-off of the filter is demonstrated on Fig. 12. This is where you see the cancelling effect of the response coming from the lasers near the different cut-offs of the optical filter. The blue and green curves are the amplitude spectra for both wavelengths (1537.07nm & 1548.44nm) one with some amplification, this is due to the fact that the detuning from the optical filter cut-off is smaller and hence the amplitude was starting to decrease. Here, the total summation of the two EM waves shows that as the amplitudes reach a same, relatively constant height, and the wave sum loses approximately 10dB from its power. This power cancellation, as written previously, is due to the  $180^\circ$  difference. There is a region in between 10-15 GHz where the system provides the cancelling effect, however it does not maintain it over the whole bandwidth of the detector, because after 15 GHz it increases again. As also shown in the RF phase transfer functions for one laser the  $180^\circ$  difference is only achieved for very specific wavelengths at each side of the optical filter cut-offs.

<http://www.photonicsbcn.eu>

**Figure 12:** Cancellation effect (in red) by weighted summation of two signals whose peaks are shown in green and blue. The vertical axis is the power measured in dB, the horizontal axis is the sweep frequency in GHz.



In this work, the optical phase transfer function of the optical filter was not looked into. For the future works, it would be convenient to characterize it and study how it could impact the results and to study ways in which its impact could be compensated. The final results gave the most optimal curves when the wavelengths were chosen from the edges of the passband of the optical filter; as it was shown on Fig. 10, 1547.07nm and 1548.44nm curves do not reach the same power level as the other wavelengths do. In summary, it is shown that cancellation happened in some limited cases, with a passband effect, however improvements can be made in order to achieve better control of the microwave filter.

### 3. DISCUSSION

As a first point of improvement, we note that the RF insertion loss of the filter was high, probably because of the lack of any kind of amplification, optical or electrical in our setup. In future tests it is advisable to consider some amplification in order to reduce the RF insertion loss.

On the other hand, analyzing the dynamic margin of the MPF would be important; the results shown here are for a 10dBm RF output power and also tests were done and with 0 and 20dBm showing no significant changes, but a systematic large signal analysis and SFDR measures are considered of great interest.

Extending the bandwidth of the experimental setup should also be considered. We used a PM capable of modulating signals up to 40 GHz and one photodetector with nominal 32 GHz bandwidth. Nevertheless the cables, connectors (SMA) and the bias-tee required for connections are only good to handle signals up to approximately 20 GHz and that can be limiting our operative frequency margin. For future measurements it is recommended to work on connection schemes that allow to extend the frequency margin of measures well beyond 30 GHz so that better results may be obtained.

Last but not least, the optical phase transfer function of the optical filter should be taken into account in the analysis to see how it may impact the phase differences observed between RF transfer functions at each side of the optical filter cut-offs. Also in this work, a single WDM channel optical filter was used and it would be interesting to try other kinds of optical filters.

### 4. CONCLUSION

The objective of this paper was to show the feasibility of a new technique for filtering in microwave photonics that has independent tunability of both ends of the RF passband of the RF filter's frequency cut-offs. The results proved the potential of the technique, which can be further improved into a more robust system by selecting circuit components, especially an optical filter, with the appropriate transfer function.

As the simulation results presented in Ref [3] introduced high hopes for such filtering technique, the paper provided the next step in a promising research area. The conducted research has revealed the key role played by the optical filter spectral transfer characteristics, and work is presently under way in order to improve the stability of the setup and to identify optical filtering structures that could help to optimize the MPF characteristics.

Universitat Politècnica de Catalunya (UPC)  
 Universitat Autònoma de Barcelona (UAB)  
 Universitat de Barcelona (UB)  
 Institut de Ciències Fotòniques (ICFO)



<http://www.photonicsbcn.eu>

**Acknowledgment.** I wish to thank UPC, the Universitat Politecnica de Catalunya for their generous support with a variety of photonical equipments and M. Santos and O. Yosefi for their thoughtful advices on microwave photonics filtering theory along the process of this work.

## REFERENCES

- [1] Jianping Yao “Photonics to the Rescue: A Fresh Look at Microwave Photonic Filters” IEEE microwave magazine, 1527-3342, September 2015, Ontario Canada
- [2] T. Chen ,X. Yi, L. Li and R. Minasian, “Single passband microwave photonic filter with wideband tunability and adjustable bandwidth”, Optics Letters Vol. 37,No 22,pp 4699-4701, Nov 2012.
- [3] O. Yosefi and M. Santos, “Compact Tunable and Reconfigurable Microwave Photonic Filter for Satellite Payloads”, International Conference on Space Optics, 2014, Tenerife Spain
- [4] A. Bensoussan and M. Vanzi, “Optoelectronic devices productassurance guideline for space application,” in Proceedings of ICSO 2010: International Conference on Space Optics (ESA, 2010), pp. 8–13.
- [5] M. Sotom, B. Benazet, A. Le Kernec, and M. Maignan, “Microwave photonic technologies for flexible satellitetelecom payloads,” in Proceedings of the 35th EuropeanConference on Optical Communication, 2009 (IEEE, 2009),pp. 20–24.
- [6] J. Capmany, J. Mora, I. Gasulla, J. Sancho, J. Lloret and S. Sales, “Microwave Photonic Signal Processing”, J. of Lightw. Technol. vol.13, no. 4, Feb 2013.
- [7] R. A. Minasian, “Photonic Signal Processing of Microwave Signals”, IEEE Trans. Microw. Theory Tech., vol.54, no. 2, Feb 2006.
- [8] J. Capmany, B. Ortega, D. Pastor, and S. Sales, “Discrete-time opticalprocessing of microwave signals,” J. Lightw. Technol., vol. 23, no. 2,pp. 702–723, Feb. 2005
- [9] X. Yi and R. A. Minasian, “Microwave Photonic Filter with single-bandpass response”, Electron.Lett.,vol. 45, No. 7, March 2009. .
- [10] D. Zhang, X. Feng and Y. Duang, “ Tunable and Reconfigurable Bandpass Microwave Photonic Filters Utilizing Integrated Optical Processor on Silicon-on-Insulator Substrate”, IEEE Photon. Technol. Lett., vol. 24, No. 17, Sept 2012.
- [11] J. Palací, G.E. Villanueva, J. V. Galan, J. Marti and B. Vidal, IEEE Photon. Technol. Lett. Vol. 22, pp. 1276 (2010).
- [12] W. Li, M. Li and J. Yao, “ A Narrow-Passband and Frequency-Tunable Microwave Photonic Filter Based on Phase-Modulation to Intensity-Modulation Conversion Using a Phase-Shifted Fiber Bragg Grating”, IEEE Trans. Microwave Th. And Tech., Vol 60, No. 5, May 2012.
- [13] VPI transmission maker, photonic modules reference manual. VirtualPhotonics Systems Inc. 2002.
- [14] B. E. A. Saleh and M. C. Teich, “Fundamentals of Photonics”, 2nd Edition, John Wiley & Sons, 2007.